

Combining SENSE and Compressed Sensing MRI With a Fast Iterative Contourlet Thresholding Algorithm

Jinpeng Zhou, Jianwu Li, Jean Claude Gombaniro

School of Computer Science and Technology
Beijing Institute of Technology
Beijing 100081

Abstract—We present a new method to improve the performance of the combination of sensitivity encoding (SENSE) and compressed sensing (CS) based on the fast iterative contourlet thresholding algorithm (FICOTA). The proposed method, dubbed as FICOTA-SENSE, separates FICOTA reconstruction and SENSE reconstruction into two sequential steps and successfully inherits the effectiveness of FICOTA. Experimental results validate that FICOTA-SENSE can provide superior performance on reconstruction quality and representation of curve-like features.

Keywords—compressed sensing, parallel imaging, SENSE, CS-SENSE, FICOTA

I. INTRODUCTION

Magnetic resonance imaging (MRI) is an essential medical imaging technology with non-invasive manner and high tissue sensitivity. However, the slow acquisition process of MRI increases its susceptibility to motion artifacts. To solve this problem, the straightforward way is to reduce the sampling. Parallel MRI (pMRI) has been widely used in both research and clinical MRI [1]. With the development of multichannel coils, pMRI can reduce the sampling workload by under-sampling and reconstruct the MR image by some standard methods: the sensitivity encoding (SENSE) [2] and the generalized auto-calibrating partially parallel acquisitions (GRAPPA) [3]. The value of theoretical maximum reduction factor can be set as the amount of coil channels, but usually this maximum is limited by the noise and imperfection in coils. A newly developed Compressed Sensing (CS) theory has been successfully applied to MRI [4-8]. The compressed sensing MRI (CS-MRI) can reconstruct MR images from significantly incomplete dataset sampled at rates lower than Nyquist criterion [9, 10].

Since both pMRI and CS-MRI accelerate MRI by reducing sampling, the combination of them can provide further acceleration. As a straightforward way, SparseSENSE and its equivalence [11-13] have combined pMRI and CS-MRI: SparseSENSE combines SparseMRI [10] with SENSE and reconstructs the final imaging by solving the same nonlinear convex optimization problem as the SparseMRI does. However, SparseSENSE replaces the Fourier encoding with sensitivity encoding. Based on this replacement, SparseSENSE has

achieved further acceleration but it cannot theoretically prove that the sensitivity encoding matrix is incoherent to any sparse transform. CS-SENSE, which can guarantee the incoherence, has been proposed as a new method for combination [1]. In CS-SENSE, the CS and SENSE are separated into two sequential steps: The first one is the CS step, which uses SparseMRI to generate a set of aliased images from the under-sampled k-space data for all the channels; second is the SENSE step, which uses SENSE to reconstruct the final unfolded image from the aliased images. The decoupling of CS and SENSE provides a superior performance on reconstruction quality to CS-SENSE. However, this improvement is limited by its CS step, which is implemented by the SparseMRI: As a pioneering work for CS-MRI, SparseMRI uses the wavelet as sparse transform and conjugate gradient (CG) method as reconstruction algorithm. However, the conventional wavelet cannot provide sparse representation of curve-like features [14] and CG has its bottleneck in computation. In [15], a fast composite splitting algorithm (FCSA) has been proposed. Though FCSA uses the same sparse transform as SparseMRI, its reconstruction algorithm has been shown to be very powerful for MRI reconstruction. It's also been proved that the combination of SENSE and FCSA is capable to improve the reconstruction accuracy [16]. Recently, a fast iterative contourlet thresholding algorithm (FICOTA) [14] has been proposed, using the contourlet [17, 18] as sparse transform and the fast iterative shrinkage-thresholding algorithm (FISTA) [19, 20] as reconstruction method.

Herein, we show a new combination of SENSE and CS, using FICOTA as the CS algorithm. Our new method, dubbed as FICOTA-SENSE, aims to provide better performance on reconstruction quality and better support for large reduction factor than CS-SENSE.

II. THEORY

A. SENSE

SENSE [2] is a standard reconstruction method for pMRI. The reconstruction model of SENSE can be defined as [21]:

$$A = Em \quad (1)$$

where A is the vector of aliased images, E is the sensitivity encoding matrix, m is the final image to be calculated. This linear equation can be formulated as a matrix form:

$$\begin{bmatrix} A_1 \\ A_2 \\ \vdots \\ A_L \end{bmatrix} = \begin{bmatrix} E_1(x, y) & \dots & E_1(x, y + (R-1)t) \\ E_2(x, y) & \dots & E_2(x, y + (R-1)t) \\ \vdots & \vdots & \vdots \\ E_L(x, y) & \dots & E_L(x, y + (R-1)t) \end{bmatrix} \begin{bmatrix} m(x, y) \\ m(x, y + t) \\ \vdots \\ m(x, y + (R-1)t) \end{bmatrix} \quad (2)$$

where (x, y) denotes the pixel position, L is the amount of receiver channels, A_i is the aliased image of the i^{th} receiver channel, R is the reduction factor, $t = \frac{n}{R}$ denotes the sampling interval and n denotes the length of y direction.

As already noted, the reduction factor R should be less than the amount of channels L . The final image m can be calculated by:

$$m = (E^H \psi^{-1} E)^{-1} E^H \psi^{-1} A \quad (3)$$

where ψ is a matrix which denotes the correlation of noise in the receiver channels, and E^H means the complex conjugate transpose of E .

B. Compressed Sensing MRI

As an emerging signal processing theory, Compressed sensing (CS) has been shown that it can be successfully applied to MRI and provide significant acceleration of acquisition process [4-10].

Define x as the MR image to be reconstructed, and F_u as an under-sampled Fourier transform. The under-sampled measurement y of x is generated by $y = F_u x$. According to the CS theory, x can be reconstructed from the measurement y because the MR images are naturally compressible. The reconstruction model can be formulated as an unconstrained regularization problem [10]:

$$\underset{x}{\operatorname{argmin}} \|F_u x - y\|_2^2 + \lambda_1 \|\Psi x\|_1 + \lambda_2 \|x\|_{TV} \quad (4)$$

where Ψ denotes a transform operator that can represent x in a sparse domain, λ_1 and λ_2 are two positive parameters for L_1 regularization and the total variation (TV) [22], respectively.

C. CS-SENSE

CS-SENSE reconstructs final image by two steps [1]. Firstly, for each channel, CS-SENSE uses the SparseMRI to generate its aliased image a from its reduced k-space data y :

$$\underset{a}{\operatorname{argmin}} \|F_u a - y\|_2^2 + \lambda_1 \|\Psi a\|_1 + \lambda_2 \|a\|_{TV} \quad (5)$$

Secondly, use the SENSE to unfold the set of aliased images, the final image can be calculated with equation (1-3).

The reduction factor R of CS-SENSE is calculated by the SparseMRI's reduction factor R_{CS} and SENSE's reduction factor R_{SENSE} :

$$R = R_{CS} \times R_{SENSE} \quad (6)$$

In [1], it has been shown that the error propagation will become serious when R_{SENSE} is larger because the noise is amplified in the step of SENSE. To minimize this noise amplification from SENSE, the R_{SENSE} should be kept in a low level.

III. RECONSTRUCTION

In this paper, the proposed combination replaces the SparseMRI component of CS-SENSE with FICOTA.

A. FICOTA

The FICOTA uses contourlet as sparse transform to improve the representation of MR images and adapts FISTA to guarantee fast computation [14]:

$$\hat{x} = \underset{x}{\operatorname{argmin}} \left\{ \frac{1}{2} \|\mathcal{F}_u x - y\|^2 + \lambda_1 \|\Phi x\|_1 \right\} \quad (7)$$

where Φ is the contourlet transform.

In algorithm 1, $f(r^k) = \frac{1}{2} \|\mathcal{F}_u r^k - y\|_2^2$ is the data consistency function, and $\nabla f(r^k) = \mathcal{F}_u^* (\mathcal{F}_u r^k - y)$ denotes the gradient of f at r^k , ρ and L_f are two positive parameters defined in [15], x^0 is initialized as zero matrix with the same size as y . Besides, FICOTA uses a 'project' function to normalize the pixel values. The L_1 regularization problem can be solved by a proximal map [19]:

$$\operatorname{prox}_\rho(g)(x) = \underset{u}{\operatorname{argmin}} \left\{ g(u) + \frac{1}{2\rho} \|u - x\|^2 \right\} \quad (8)$$

where $g(x)$ is a continuous convex function.

Algorithm 1 FICOTA [14]

INPUTS: $\rho = 1/L_f, \lambda_1; r^1 = x^0; t^1 = 1$

for $k = 1 : \maxIter$

$x_g = r^k - \rho \nabla f(r^k);$

$x^k = \operatorname{prox}_\rho(2\lambda_1 \|\Phi x\|_1)(x_g)$

$x^k = \operatorname{project}(x^k, [l, u]);$

$t^{k+1} = \frac{1 + \sqrt{1 + 4(t^k)^2}}{2};$

$r^{k+1} = x^k + \frac{t^k - 1}{t^{k+1}}(x^k - x^{k-1});$

end

B. FICOTA-SENSE

The proposed FICOTA-SENSE reconstruction includes two steps: (a) generating each channel's aliased image from its under-sampled k-space data using FICOTA, (b) unwrapping all the aliased images to reconstruct the final result using SENSE. The scheme of our combination is shown in Fig. 1.

Similar to CS-SENSE, the reconstruction model in the first step of FICOTA-SENSE can be formulated as:

$$\underset{a}{\operatorname{argmin}} \left\{ \frac{1}{2} \|\mathcal{F}_u a - y\|^2 + \lambda_1 \|\Phi a\|_1 \right\} \quad (9)$$

In the second step, FICOTA also uses SENSE to unfold the aliased images a to generate the final result.

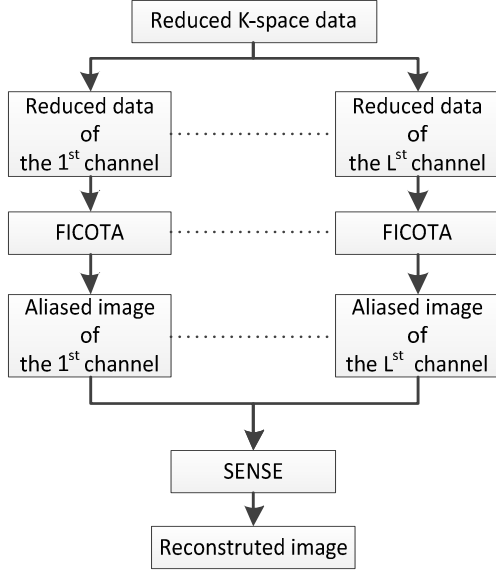


Figure 1. The scheme of FICOTA-SENSE

IV. EXPERIMENTS

We performed our experiments on a MRI dataset `mprage_8ch_slice1.mat` [23] and implemented SENSE using the toolbox PULSAR [24]. The proposed combination, FICOTA-SENSE, was compared to the CS-SENSE. Besides, to evaluate the performance of FICOTA in the combination, we also implemented a simple combination of SENSE and FCSA using the same scheme as FICOTA-SENSE, except that we replace the FICOTA parts with FCSA. This combination of SENSE and FCSA here is dubbed as FCSA-SENSE. There are three basic steps to reconstruct final image from the original MRI dataset.

Firstly, to acquire the under-sampled data, we sampled the k-space in phase encoding direction with a reduction factor of SENSE to get the reduced k-space data. Then we further under-sampled the reduced k-space data using a variable-density random sampling pattern with a reduction factor of CS.

Secondly, to generate all the aliased images, we used FICOTA, FCSA and SparseMRI as the CS algorithms, respectively. The CS sparse transform in our experiments varied with the CS algorithms: we used a sharp frequency localization contourlet [18] for FICOTA-SENSE and the Daubechies-4 wavelet for CS-SENSE and FCSA-SENSE.

Finally, to reconstruct the final image, we used SENSE to unfold the aliased images. The sensitivity encoding matrix for SENSE was calculated from the central 32 phase encoding lines which are fully sampled in k-space.

In our experiments, we did the comparison for an overall reduction factor R of 4, 6, 8 and 10. To avoid the noise amplification, we kept the reduction factor of SENSE $R_{SENSE} = 2$ for each simulation.

For CS-SENSE, we set the same regularization parameters for SparseMRI as the original values [10]. For

FICOTA-SENSE, we set the parameter λ_2 as 0.0015. For each method, we add a Gaussian white noise to the k-space data y with a standard deviation 0.01.

To evaluate and compare the performance of different combinations, we used the transferred edge information (TEI) [25], the peak SNR (PSNR), the normalized mean square error (NMSE) [26] and the correlation coefficients (CC) as criterions, and for comparison, we also used the sum-of-squares (SoS) method to generate an image from fully sampled data as the reference image.

TABLE I. COMPARISONS OF DIFFERENT METHODS

Methods	R	Criterions			
		CC	NMSE	PSNR	TEI
CS-SENSE	4	0.9957	0.0034	77.433	0.7120
	6	0.9901	0.0078	73.802	0.5856
	8	0.9841	0.0125	71.745	0.4866
	10	0.9785	0.0169	70.445	0.4259
FCSA-SENSE	4	0.9950	0.0043	76.427	0.6849
	6	0.9905	0.0077	73.860	0.5645
	8	0.9869	0.0104	72.554	0.4852
	10	0.9811	0.0151	70.931	0.4190
FICOTA-SENSE	4	0.9979	0.0017	80.410	0.7961
	6	0.9957	0.0034	77.390	0.7182
	8	0.9929	0.0056	75.217	0.6550
	10	0.9897	0.0082	73.589	0.6075

Table 1 summarizes the results of comparison based on the chosen criterions with different overall reduction factor R for different methods. Fig. 2 shows the reconstructed images based on different combinations. Fig. 3 shows the plots of PSNR versus the overall reduction factors. Fig. 4 shows the plots of TEI versus the overall reduction factors.

According to Fig. 2, FICOTA-SENSE provides better image quality than FCSA-SENSE and CS-SENSE and improves the representation of curve-like features.

According to Fig. 3, FICOTA-SENSE sacrifices less resolution for acceleration and provides better performance

than FCSA-SENSE and CS-SENSE when the overall reduction factor is large.

According to Fig. 4, FICOTA-SENSE provides better results in TEI, which means it can provide better performance on edge strength and orientation preservation.

Furthermore, according to Table 1, the proposed methods outperform the CS-SENSE in term of four criterions.

V. CONCLUSION

This paper proposes a new combination of FICOTA and SENSE to improve the reconstruction quality of the combination of CS and SENSE. Experimental results have shown our proposed method not only can improve both

efficiency and precision, but also can provide better support for a large reduction factor than the original CS-SENSE. Furthermore, FICOTA-SENSE can improve the representation of curve-like features.

The combination of CS-MRI and pMRI has been shown to be useful in MR image reconstruction, especially when the k-space data is highly under-sampled. Further effort is needed to investigate the combination of more advanced CS and pMRI methods to improve reconstruction effectiveness.

ACKNOWLEDGMENT

This work was supported by the National Natural Science Foundation (NNSF) of China (No. 61271374).

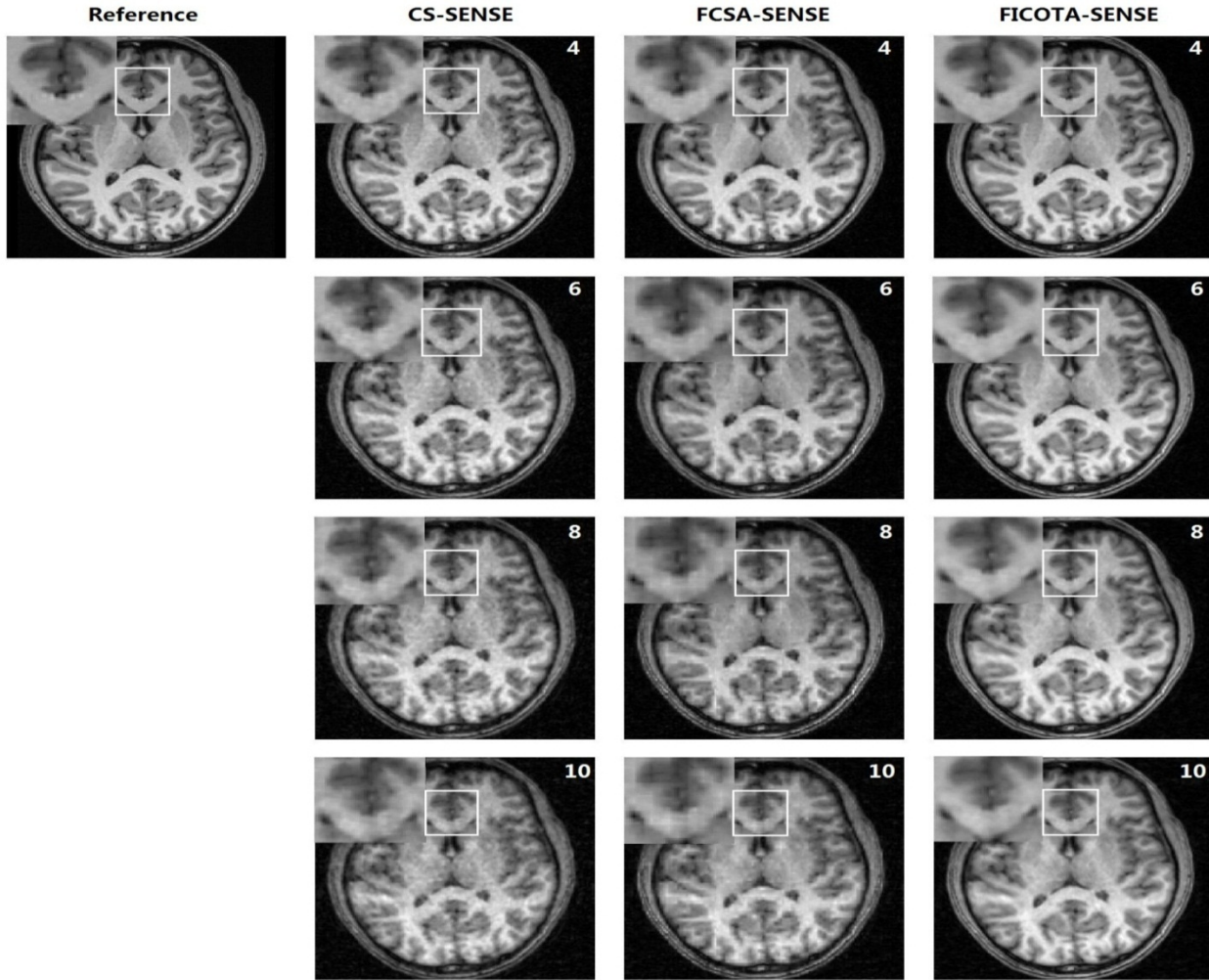


Figure 2. Reconstructed images with their overall reduction factors shown on the top right corner of each image

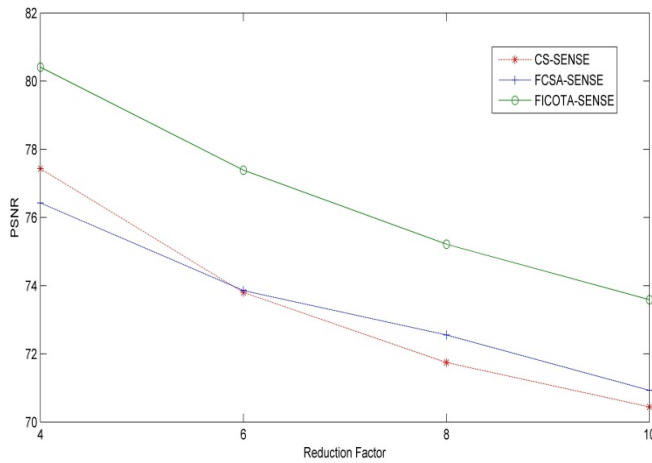


Figure 3. PSNR versus the overall reduction factor

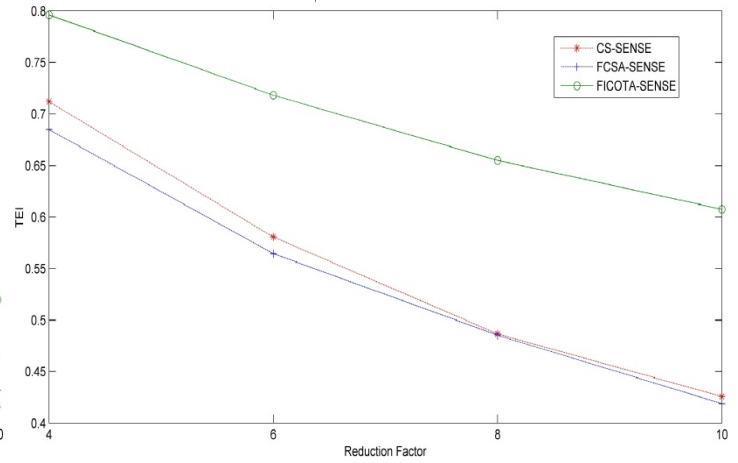


Figure 4. TEI versus the overall reduction factor

REFERENCES

- [1] Liang, D., Liu, B., Wang, J., and Ying, L.: Accelerating SENSE using compressed sensing. *Magnetic Resonance in Medicine*, 2009, 62, (6), pp. 1574-1584.
- [2] Pruessmann, K.P., Weiger, M., Scheidegger, M.B., and Boesiger, P.: SENSE: sensitivity encoding for fast MRI. *Magnetic Resonance in Medicine*, 1999, 42, (5), pp. 952-962.
- [3] MA, G., PM, J., RM, H., M, N., V, J., J, W., B, K., and A, H.: Generalized autocalibrating partially parallel acquisitions (GRAPPA). *Magnetic Resonance in Medicine*, 2002, 47, (6), pp. 1202-1210.
- [4] Donoho, D.L.: Compressed sensing. *IEEE Trans. On Information Theory*, 2006, 52, (4), pp. 1289-1306.
- [5] Tsaig, Y., and Donoho, D.L.: Extensions of compressed sensing. *Signal Process*, 2006, 86, (3), pp. 549-571.
- [6] Candès, E.J.: Compressive sampling. *Proceedings of the International Congress of Mathematicians*, 2006, pp. 1433-1452.
- [7] Baraniuk R.: Compressive sensing. *IEEE Signal Processing Magazine*, 2007, 24,(4), pp.118-121.
- [8] Candès E J, Wakin M B.: An introduction to compressive sampling. *Signal Processing Magazine, IEEE*, 2008, 25m (2), pp. 21-30.
- [9] Lustig, M., Donoho, D.L., Santos, J.M., and Pauly, J.M.: Compressed Sensing MRI. *Signal Processing Magazine, IEEE*, 2008, 25, (2), pp. 72-82.
- [10] Lustig, M., Donoho, D., and Pauly, J.M.: Sparse MRI: The application of compressed sensing for rapid MR imaging. *Magnetic Resonance in Medicine*, 2007, 58, (6), pp. 1182-1195.
- [11] Liu, B., Seibert, F.M., Zou, Y., and Ying, L.: SparseSENSE: randomly-sampled parallel imaging using compressed sensing. 16th Annu. Meeting of ISMRM (Toronto, Canada 2008), pp. 3154.
- [12] Zhao C, Lang T, Ji J.: Compressed sensing parallel imaging. 16th Annu. Meeting of ISMRM (Toronto, Canada 2008), pp. 1478.
- [13] King K F, Angelos L.: SENSE with partial Fourier homodyne reconstruction. 8th Annual Meeting of ISMRM (Denver, USA 2000), pp. 153.
- [14] Hao, W., Li, J., Qu, X., and Dong, Z.: Fast iterative contourlet thresholding for compressed sensing MRI. *Electronics Letters*, 2013, 49, (19), pp. 1206-1208.
- [15] J, H., S, Z., and D, M.: Efficient MR image reconstruction for compressed MR imaging. *Medical Image Analysis*, 2011, 15, (5), pp. 670-679.
- [16] Jiang, M., Jin, J., Liu, F., Yu, Y., Xia, L., Wang, Y., and Crozier, S.: Sparsity-constrained SENSE reconstruction: An efficient implementation using a fast composite splitting algorithm. *Magnetic Resonance Imaging*, 2013, 31, (7), pp. 1218-1227.
- [17] M.N. Do and M. Vetterli: The contourlet transform: An efficient directional multiresolution image representation, *IEEE Trans. Image Procession*. 14(2005), pp.2091-2106.
- [18] Lu Y., Do M. N.: A New Contourlet Transform with Sharp Frequency Localization, *Image Processing*, 2006 IEEE International Conference on. IEEE, 2006, pp. 1629-1632.
- [19] Beck, A., and M, T.: A fast iterative shrinkage-thresholding algorithm for linear inverse problems. *SIAM J. Imaging Sci.*, 2009, 2, (01), pp. 183-202.
- [20] Beck, A., and Teboulle, M.: 'Fast gradient-based algorithms for constrained total variation image denoising and deblurring problems', *IEEE Trans. Image Procession*, 2009, 18, (11), pp. 2419-2434.
- [21] Pruessmann KP, Weiger M, Börnert P.: Advances in sensitivity encoding with arbitrary k-space trajectories. *Magnetic Resonance Medicine*, 2001, 46, pp. 638 - 651.
- [22] Rudin L, Osher S, Fatemi E.: Non-linear total variation noise removal algorithm. *Phys D* 1992, 60 , pp. 259 - 268.
- [23] http://www.nmr.mgh.harvard.edu/~fhlin/codes/mprage_8ch_slice1.mat
- [24] Ji J X, Son J B and Rane S D: PULSAR: A Matlab toolbox for parallel magnetic resonance imaging using array coils and multiple channel receivers Concepts Magn. Reson. B; *Magnetic Resonance Engineering*. 2007, 31B, pp. 24-36.
- [25] X. Qu, W. Zhang, D. Guo, C. Cai, S. Cai, and Z. Chen: Iterative thresholding compressed sensing MRI based on contourlet transform. *Inverse Problems in Science and Engineering*, 2010, vol. 18, pp. 737-758,.
- [26] Ying L, Sheng J.: Joint image reconstruction and sensitivity estimation in SENSE (JSENSE). *Magnetic Resonance Medicine* 2007, 57, pp. 1196 - 1202.